Temporal differentiation of optical signals using a phase-shifted fiber Bragg grating

Naum K. Berger, Boris Levit and Baruch Fischer

Department of Electrical Engineering, Technion - Israel Institute of Technology, Haifa 32000, Israel.
chrberg@techunix.technion.ac.il

Mykola Kulishov* and David V. Plant

Department of Electrical and Computer Engineering, McGill University, Montréal, Québec H3A 2A7, Canada
** He is now with HTA Photomask Inc., San Jose, CA, 95131, USA*
mykolak@htaphotomask.ca

José Azaña

Institut National de la Recherche Scientifique (INRS), Montréal, Québec H5A 1K6, Canada
azana@emt.inrs.ca

Abstract: We propose and experimentally demonstrate an all-optical (all-fiber) temporal differentiator based on a simple π-phase-shifted fiber Bragg grating operated in reflection. The proposed device can calculate the first time derivative of the complex field of an arbitrary narrowband optical waveform with a very high accuracy and efficiency. Specifically, the experimental fiber grating differentiator reported here offers an operation bandwidth of ≈ 12 GHz. We demonstrate the high performance of this device by processing gigahertz-bandwidth phase and intensity optical temporal variations.

OCIS codes: (060.2340) Fiber optics components; (200.3050) Information processing; (230.1150) All-optical devices; **(**320.5540) Pulse shaping; (999.9999) Fiber Bragg gratings.

References and links

1. J. Azaña, C. K. Madsen, K. Takiguchi, and G. Cincontti, eds., "Optical Signal Processing," J. Ligthwave Technol. **24**, 2484-2767 (2006).
2. N. Q. Ngo, S. F. Yu, S. C. Tjin, and C.H. Kam, "A new theoretical basis of higher-derivative optical differentiators," Opt. Commun. **230**, 115-129 (2004).
3. M. Kulishov, and J. Azaña, "Long-period fiber gratings as ultrafast optical differentiators," Opt. Lett. **30**, 2700-2702 (2005).
4. R. Slavík, Y. Park, M. Kulishov, R. Morandotti, and J. Azaña, "Ultrafast all-optical differentiators," Opt. Express **14**, 10699-10707 (2006).
5. R. Kashyap, *Fiber Bragg Gratings*, (Academic Press, San Diego, 1999).
6. A. Othonos and K. Kalli *Fiber Bragg Gratings. Fundamentals and Applications in Telecommunications and Sensing*, (Artech House, Boston, 1999).
7. H. J. A. Da Silva, and J. J. O'Reilly, "Optical pulse modeling with Hermite - Gaussian functions," Opt. Lett. **14**, 526-528 (1989).
8. A. Papoulis, *The Fourier Integral and its Applications*, (McGraw-Hill, New York 1987).
9. M. Yamada, and K. Sakuda, "Analysis of almost-periodic distributed feedback slab waveguides via a fundamental transfer matrix approach," Appl. Opt. **26**, 3474-3478 (1987).
10. J. E. Bjorkholm, E. H. Turner, and D. B. Pearson, "Conversion of cw light into a train of subnanosecond pulses using frequency modulation and the dispersion of a near-resonant atomic vapor," Appl. Phys. Lett. **26**, 564-566 (1975).
11. N. K. Berger, B. Levit, and B. Fischer, "Complete characterization of optical pulses using a chirped fiber Bragg grating," Opt. Commun. **251**, 315-321 (2005).
12. M. Takeda, H. Ina, and S. Kobayashi, "Fourier-transform method of fringe-pattern analysis for computer-based topography and interferometry," J. Opt. Soc. Am. **72,** 156–160 (1982).

#75835 - $15.00 USD Received 12 October 2006; revised 6 December 2006; accepted 12 December 2006

1. Introduction

The implementation of all-optical circuits for computing and networking could overcome the speed limitations associated with conventional electronics implementations [1]. A potential alternative to achieve this general goal is to try to emulate the developments in the electronic domain using all-optical technologies. For this purpose, photonics equivalents of fundamental devices that form basic building blocks in electronic circuits would need to be designed and implemented. A temporal differentiator is one of these fundamental devices. Several schemes for performing real-time derivation of arbitrary signals in the optical domain have been previously proposed at the theoretical level [2], [3]. For instance, very recently, it has been shown that a uniform long-period fiber grating (LPG) operating in full-coupling condition implements a first-order time differentiator over arbitrary optical signals with sub-picosecond temporal features [3]. An important requirement in this approach is that the signals to be differentiated must be spectrally centered at the LPG resonance frequency. Based on this finding LPG optical differentiators capable of processing signals with temporal features as fast as $\approx$ 180 fs have been fabricated and experimentally tested [4]. The LPG-based solution is specially suited for differentiating optical waveforms with bandwidths > 100-GHz [3]. However this previous solution is very energetically inefficient for processing optical signals with bandwidths in the GHz regime since most of the signal energy lying within a bandwidth of a few GHz around the LPG resonance frequency is filtered out by the grating filter. Another well-known drawback of an LPG solution is its extreme sensitivity to environmental (e.g. temperature) fluctuations.

In this letter, we propose and experimentally demonstrate a new all-optical differentiation approach, which allows us to overcome the typical limitations of the LPG-approach and in particular, it is ideally suited for operation on optical signals with bandwidths up to a few GHz. Specifically, we demonstrate that a single π phase-shifted fiber Bragg grating (FBG) [5], [6] operated in reflection can accurately and efficiently calculate the first time derivative of the complex field (amplitude and phase) of a GHz-bandwidth arbitrary input optical waveform. Advantages of the realized device are inherent to all-fiber geometries and include simplicity, relatively low cost, low losses, polarization independence and full compatibility with fiber optics systems.

Besides the intrinsic interest of an optical temporal differentiator for all-optical information processing, the device could be readily applied for optical pulse re-shaping operations [2], [7] or for optical sensing and control (e.g. for finding maxima or minima or points of greatest slope in an ultrafast signal that carries information about a system to be diagnosed [2]). As they can alleviate the bandwidth limitations typical of electronic solutions, the reported devices are also attractive for realizing specific signal processing operations over ultra-wideband microwave signals (by first transferring the microwave signal into the optical domain using e.g. electro-optic modulation).

2. Operation principle

The spectrum associated with the derivative of the temporal envelope of a given signal centered at frequency ω_0 (carrier frequency) $E(\omega-\omega_0)$ (represented in the Fourier domain) is given by $i(\omega-\omega_0)E(\omega-\omega_0)$ [8], where ω is the optical frequency, and $\omega-\omega_0$ is the base-band frequency. Thus, a first-order temporal differentiator is essentially a linear filtering device providing a spectral transfer function of the form $H(\omega-\omega_0) = i(\omega-\omega_0)$. Consequently, the two key features of the filter's transmission are (i) it depends linearly on the base-band frequency, and (ii) it is zero at the signal central frequency ω_0. It is worth noting that these two key features imply an exact π phase shift across the central frequency ω_0.

We demonstrate here that the required spectral features of a temporal differentiator are inherently provided by the reflection response of a suitable phase-shifted uniform FBG over a limited bandwidth around the grating Bragg wavelength, i.e. within the reflection resonance dip. A phase-shifted FBG consists of two concatenated uniform FBGs with a phase shift φ

#75835 - $15.00 USD Received 12 October 2006; revised 6 December 2006; accepted 12 December 2006

between them. This structure can be described using the transfer matrix method [9]. Specifically, the transfer (2×2) matrix $\mathbf{T_{ps}}$ of a phase-shifted FBG can be written as

$$\mathbf{T_{ps}} = \mathbf{T_1}\cdot\mathbf{T_\varphi}\cdot\mathbf{T_2} \tag{1}$$

where $\mathbf{T_1}$, $\mathbf{T_2}$, and $\mathbf{T_\varphi}$ are the 2×2 matrices of the two uniform Bragg gratings and of the phase shift between the gratings, respectively. The elements of the transfer matrix corresponding to each uniform Bragg grating section are [9]:

$$T_{m11} = T_{m22}^{\ *} = [\cosh(\gamma_m l_m)+i(\delta\beta)l_m\sinh(\gamma_m l_m)/(\gamma_m l_m)]\exp(i2\pi n_{eff}l_m/\lambda_B), \tag{2}$$

$$T_{m12} = T_{m21}^{\ *} = -[k_m l_m\sinh(\gamma_m l_m)/(\gamma_m l_m)]\ \exp(-i2\pi n_{eff}l_m/\lambda_B), \tag{3}$$

where $\gamma_m^{\ 2} = k_m^{\ 2} - (\delta\beta)^2$. In the above expressions, the symbol * denotes complex conjugation, m = 1, 2 refers to the number of the grating, k_m is the coupling coefficient of the m-th grating, l_m is the corresponding grating length, $\delta\beta = 2\pi n_{eff}(\lambda^{-1}-\lambda_B^{-1})$ is the detuning from the Bragg wavelength λ_B (which is assumed to be the same for the two uniform sections), and n_{eff} is the effective fiber mode index. The elements of the transfer matrix corresponding to the phase shift φ are [5]:

$$T_{\varphi 11} = \exp(-i\varphi/2);\ T_{\varphi 22} = \exp(i\varphi/2);\ T_{\varphi 12} = T_{\varphi 21} = 0 \tag{4}$$

The field reflectivity r and transmittance τ of a Bragg grating structure can be found from its transfer matrix **T** as

$$r = \frac{T_{21}}{T_{11}} \tag{5}$$

$$\tau = \frac{1}{T_{11}} \tag{6}$$

Specifically, the field reflectivity of a phase-shifted FBG can be obtained from the elements of the transfer matrix $\mathbf{T_{ps}}$ given by Eq. (1) using the relations in Eq. (5) and Eq. (6):

$$r_{ps} = \frac{r_1 + r_2\exp[i(\varphi + 2\varphi_{1\tau})]}{1+r_1^{*}r_2\exp[i(\varphi + 2\varphi_{1\tau})]} \tag{7}$$

where r_1 and r_2 are the field reflectivities of the first and second uniform Bragg grating, respectively; these reflectivities can be found from the corresponding individual matrix elements [expressions given in Eq. (2) and Eq. (3)] using the relation in Eq. (5). $\varphi_{1\tau}$ is the phase acquired by transmission through the first uniform Bragg grating, which can be obtained from the corresponding transmission coefficient τ_1 using Eq. (6). The intensity reflectivity R_{ps} and reflection phase θ_{ps} of the phase-shifted FBG are obtained from Eq. (7), and in particular, $R_{ps} = |r_{ps}|^2$ and $\theta_{ps} = \arg(r_{ps})$.

The phase shift in the otherwise uniform FBG structure causes a resonance-induced transmission peak (i.e. reflection dip) in the grating's spectral transmission bandgap (reflection spectral band) [5]. In what follows we will show by numerical simulations that if certain conditions are satisfied, then the grating's reflection dip exhibits the precise spectral characteristics that are required for optical differentiation. We recall that these characteristics involve an amplitude response that depends linearly on the frequency variable with a complex zero at the central frequency. The specific required conditions for optical differentiation are: (i) the two uniform FBGs in the structure must be identical ($l_1 = l_2 = L$, and $k_1 = k_2 = k$), i.e. $r_1 = r_2 = r$, and (ii) the phase shift in the middle of the structure must be exactly $\varphi = \pi$. If these two conditions are satisfied the reflection coefficient in Eq. (7) is simplified to:

#75835 - $15.00 USD Received 12 October 2006; revised 6 December 2006; accepted 12 December 2006

$$r_{ps} = \frac{r[1-\exp(2i\varphi_{1\tau})]}{1-|r|^2\exp(2i\varphi_{1\tau})} \tag{8}$$

Figure 1 shows the numerically simulated field reflectivity $|r_{ps}|$ and phase θ_{ps} of an ideal π phase-shifted uniform FBG that satisfies the above conditions. Specifically, the simulated structure is composed by two identical concatenated uniform FBGs, each with a length $l_1 = l_2 = L \approx 1$ mm, Bragg wavelength $\lambda_B = 1550$ nm, and effective refractive index $n_{eff} = 1.46$, and with an exact π phase shift between the two uniform grating sections. Notice that the length of each uniform grating was fixed to be an exact integer multiple of the grating period $\Lambda = \lambda_B/(2n_{eff})$, i.e. $L = N\cdot\Lambda$, with N = 1884. This ensures that the minimum of reflectivity is located exactly at the Bragg wavelength [as shown in Fig. 1(a)]; the effect of deviation from this condition is simply a shift in the wavelength of minimum reflectivity (relative to the Bragg wavelength). Figure 1 demonstrates that the reflection response of this FBG structure provides the desired amplitude and phase features for optical differentiation over a relatively narrow bandwidth around the Bragg frequency (within the grating reflection dip). As a result, this simple device could be used to calculate the first time derivative of an arbitrary optical signal centered at the grating Bragg (resonance) frequency ($\omega_0 = \omega_B$) assuming that this signal exhibits a bandwidth narrower than the spectral linear region in the grating reflection dip.

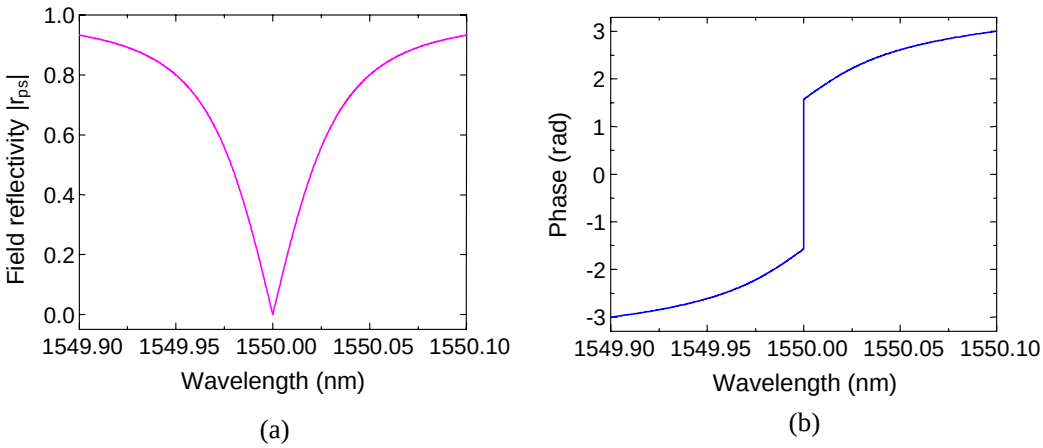

Fig. 1. Numerically simulated (a) field reflectivity and (b) phase of an ideal π phase-shifted FBG around its reflection resonance dip.

It is well known that FBGs are less sensitive to environmental (e.g. temperature) variations than LPGs. Similarly to any FBG structure, in our device, temperature changes will affect both the refractive index (thermo-optic effect) and the periodic space between grating planes (thermo-elastic effect) [6]. Given that the spacing between the two concatenated FBGs in our structure is nearly zero, temperature variations should induce only a Bragg wavelength shifting in the FBG filter, which according to previous estimations should be ≈13.7 pm/°C (for λ=1550 nm) [6].

3. Numerical analysis of a practical π phase-shifted FBG

According to our analysis above, a phase-shifted FBG operated in reflection can provide the ideal spectral features that are required for optical differentiation if the following conditions are satisfied: (i) the FBG must exhibit a phase shift of π exactly located at the center of the grating structure; and (ii) the two uniform FBGs surrounding this π phase shift must be identical in grating period, length and coupling strength. In practice, deviations from these

#75835 - $15.00 USD Received 12 October 2006; revised 6 December 2006; accepted 12 December 2006

ideal conditions should be expected and this should affect the device operation as an optical differentiator. In what follows, we present numerical simulations to evaluate the impact of these potential non-idealities in a practical optical differentiation experiment. The effect of deviation from any of the above mentioned ideal conditions in the grating spectral response is very similar and in particular, a non-zero resonance dip should be expected in a practical grating. In order to emulate this situation, in our simulations we have assumed that the two concatenated uniform FBGs have a slightly different coupling coefficient so that a resonance dip of -30dB is achieved in the grating reflection response (this is very close to what we can achieve in practice with our grating fabrication setup).

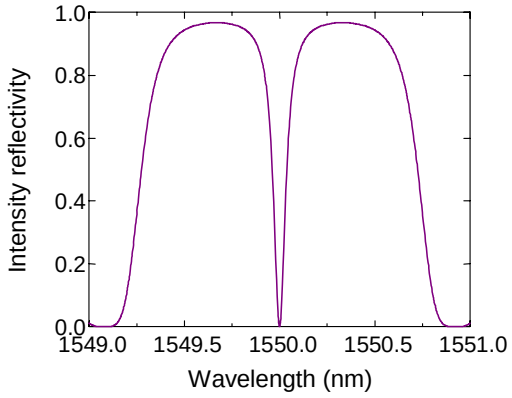

Fig. 2. Calculated intensity reflectivity of the non-ideal phase-shifted fiber Bragg grating.

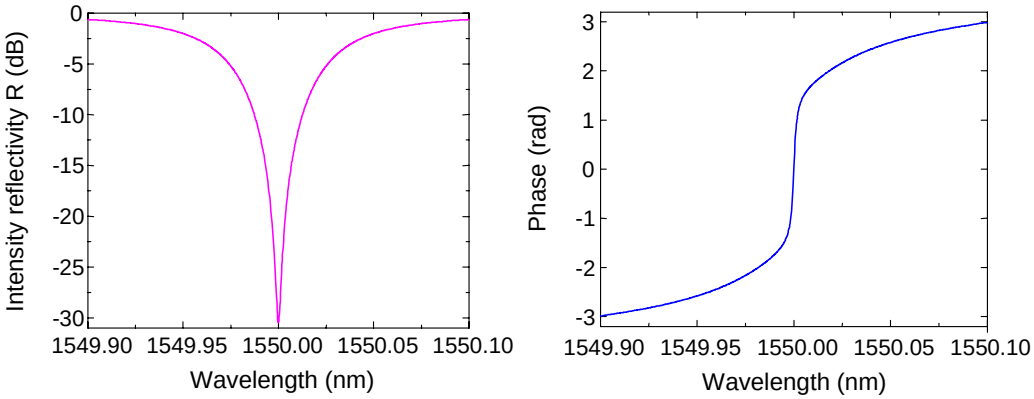

Fig. 3. Calculated (a) reflection spectral dip (logarithmic scale) and (b) reflection spectral phase response of the non-ideal phase-shifted fiber Bragg grating.

In the simulations presented here, we assumed an exact π phase shift at the center of the grating structure and we used the following parameters for the uniform gratings: $L = l_1 = l_2 \approx 1$ mm ($L = N \cdot \Lambda$, with $N = 1884$), $\lambda_B = 1550$ nm, and $n_{eff} = 1.46$. The intensity reflectivity of the numerically simulated π-phase-shifted Bragg grating is shown in Fig. 2. For these simulations, we used the transfer matrix method described above. As expected, the reflection response at the Bragg frequency is close to zero and a frequency linear dependence of this reflection

#75835 - $15.00 USD Received 12 October 2006; revised 6 December 2006; accepted 12 December 2006

response can be observed over a narrow bandwidth around this resonance frequency. A logarithmic representation of this intensity reflectivity over a bandwidth of 0.2 nm around the resonance frequency [Fig. 3(a)] shows that the reflectivity at this resonance frequency is however not exactly 0 (as anticipated, a resonance dip of ≈ -30dB is achieved). Similarly, while an exact discrete π phase-shift is expected at the resonance frequency in the reflection spectral response of an ideal FBG structure, in practice (e.g. when the concatenated uniform gratings exhibit a different coupling strength or length) the obtained spectral phase jump is not abrupt [see simulation results in Fig. 3(b)]. We recall that the discrete π phase-shift at the central frequency is an essential feature to achieve optical differentiation.

As for the optical signal to be differentiated, we assumed the same method of optical pulse generation as in the performed experiments. Specifically, CW laser radiation ($\lambda_0 = \lambda_B$ = 1550 nm) was first sinusoidally phase modulated and then propagated in a dispersive optical fiber [10]. In our calculations, we used the following parameters: modulation frequency f_m = 1 GHz, modulation index A = 2.405 rad, and fiber dispersion DL = -4074 ps/nm. The intensity of the obtained 1-GHz optical pulse train and the corresponding discrete energy spectrum are shown in Fig. 4 (a) and Fig. 4 (b), respectively.

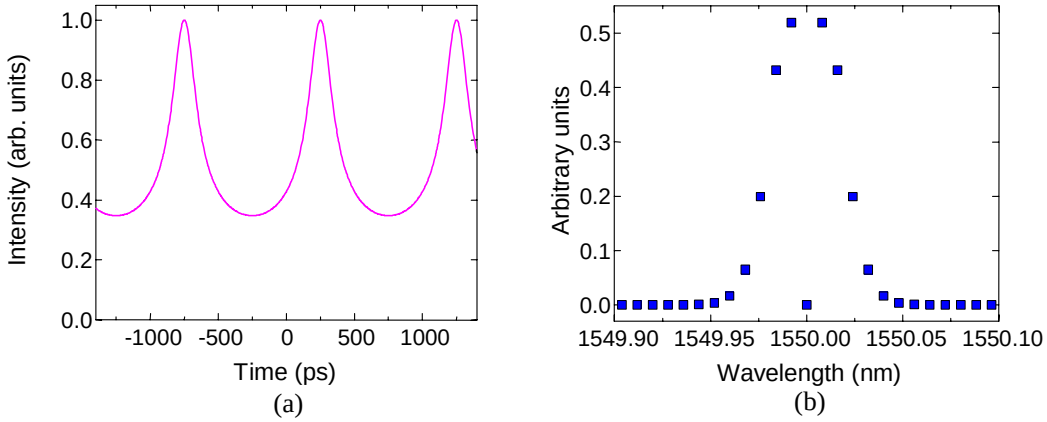

Fig. 4. Calculated (a) temporal intensity and (b) discrete energy spectrum of the periodic input optical pulses.

In Fig. 5, we compare the exact differentiation of the optical pulses shown in Fig. 4 and the approximate differentiation obtained by reflection of these pulse from the simulated phase-shifted fiber Bragg grating having the characteristics presented in Fig. 2 and Fig. 3. Specifically, the red curve in Fig. 5 shows the squared magnitude of the first time derivative of the input signal (pulse train) field whereas the blue curve in Fig. 5 shows the intensity of the pulses reflected from the phase-shifted FBG. There is an excellent agreement between these two curves and in particular, the calculated relative average deviation between the two curves is ≈ 7%. This clearly confirms that a practical phase-shifted Bragg grating (with a resonance dip of at least -30-dB) could be successfully used for accurate and efficient temporal pulse differentiation of GHz-bandwidth optical signals.

#75835 - $15.00 USD Received 12 October 2006; revised 6 December 2006; accepted 12 December 2006

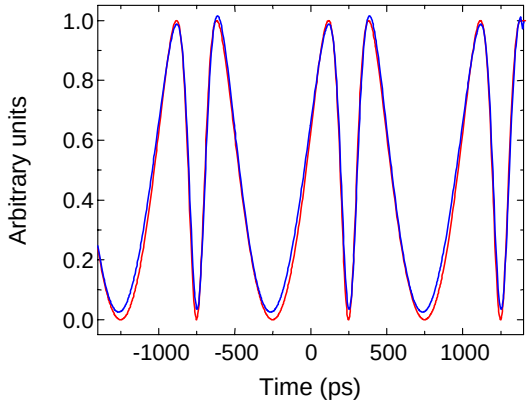

Fig. 5. Calculated squared magnitude of the first time derivative (red curve) of the pulses shown in Fig. 4 and calculated temporal intensity of the pulses reflected from the phase-shifted Bragg grating (blue curve).

4. Fabrication and characterization of a phase-shifted FBG-based optical differentiator

A phase-shifted Bragg grating was fabricated using the UV radiation from a CW frequency doubled Ar-ion laser with power of about 160 mW. The UV beam was focused by a cylindrical lens trough a 1 mm slit and a phase mask with a period of 1065 nm onto the core of a hydrogen-loaded germanosilicate fiber. The written phase-shifted grating consists of two consecutive ≈1 –mm long uniform FBGs. The π-phase shift between the two parts of the grating was produced by the displacement of the mask relative to the fiber using a piezoelectric actuator after the first grating was written. The spectral reflectivity of the fabricated grating was measured by a tunable semiconductor laser (Ando AQ4321D) and an optical spectrum analyzer (Ando AQ6317B) with a wavelength resolution of 1 pm. The measured reflection spectrum is shown in Fig. 6(a). Notice that in Fig. 6(a), we only show the reflectivity around the resonance dip as this is the region of the grating spectral response that is relevant for optical differentiation. The resonance dip was centered at λ_B = 1542.15 nm, and exhibited a depth of -34.5 dB and a 3-dB bandwidth of 0.17 nm.

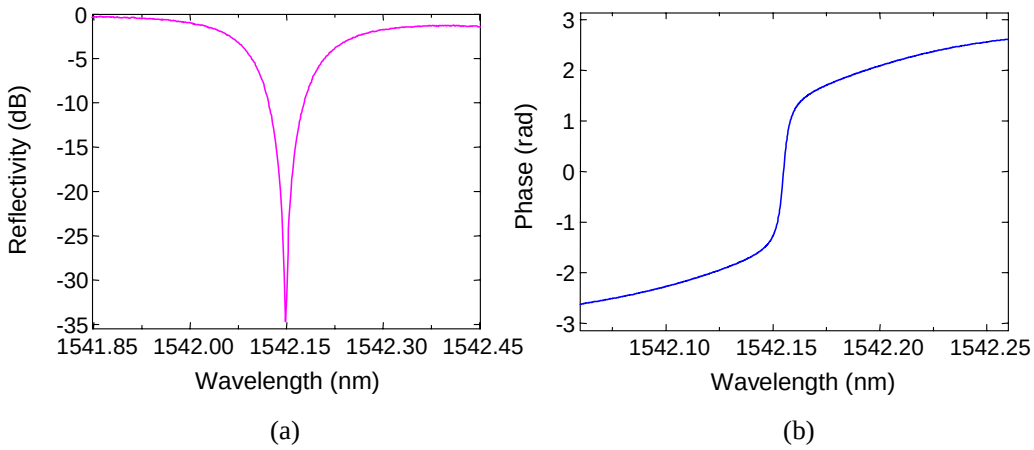

Fig. 6. Measured (a) spectral reflectivity and (b) reflection phase response of the fabricated phase-shifted FBG.

The grating spectral phase in reflection was also measured; for this purpose, we used the method described in Ref. [11]. The phase-shifted FBG was placed in one of the arms of an all-fiber Michelson interferometer. The spontaneous emission of an EDFA was reflected both

#75835 - $15.00 USD Received 12 October 2006; revised 6 December 2006; accepted 12 December 2006

from the grating to be characterized and from the reference mirror of the interferometer – the two reflected signals were made to interfere and the resultant spectral interference pattern was recorded by an optical spectrum analyzer. We then used a phase retrieval procedure similar to that described in Ref. [12] for spatial interference measurements. Briefly, we first calculated the Fourier transform of the recorded interference pattern. It consists of a central band and two symmetrical sidebands. The path difference in the interferometer and, accordingly, the oscillation frequency in the interference pattern were fixed to ensure that these 3 bands were separated. One of the sidebands was first extracted out and then shifted to zero. This corresponds to eliminating the linear component in the wavelength dependence of the reflection phase. Then, the shifted band was inverse Fourier transformed and the grating phase spectral response was calculated as the argument of the resultant signal from this last Fourier transformation. Finally, a linear phase component corresponding to a very weak grating with a length of 2 mm was added to the originally recovered phase and in this way, we found the complete phase spectral response of the phase-shifted FBG. The measured spectral phase response is shown in Fig. 6(b). As expected, a relatively abrupt phase shift (close to π) was measured at the resonance wavelength of 1542.15 nm.

5. Experimental results and discussions

The operation of the fabricated phase-shifted fiber Bragg grating as an optical differentiator was tested using the experimental setup shown in Fig. 7. As an optical source, we used the same tunable semiconductor laser as for the grating spectrum measurement. This laser was tuned for operation at the FBG resonance frequency ($\lambda_0 = \lambda_B = 1542.15$ nm). The CW radiation from the laser was sinusoidally modulated by a $LiNbO_3$ electro-optic phase modulator driven by a RF signal supplied by a RF synthesizer followed by an RF amplifier.

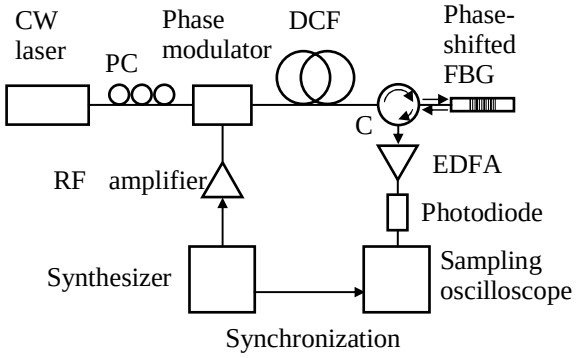

Fig. 7. Experimental setup for optical signal differentiation: PC – polarization controller, DCF – dispersion compensating fiber, C – circulator, EDFA – erbium doped fiber amplifier.

It is very important to emphasize that the proposed optical differentiation technique provides the first time derivative of the complex field of the input optical signal (not the derivative of the signal intensity). This implies that even for pure phase modulation, we are able to observe the results of optical differentiation. In order to illustrate this important aspect, we carried out two sets of experiments. In the first set, we used sinusoidally phase modulated laser light (with a constant temporal intensity) as the input signal to be differentiated. In the second set of experiments, we used as an input optical signal a pulse train that was generated by propagating the sinusoidally phase modulated light through a dispersive fiber (see simulations above). In this case, the phase as well as the intensity of the input pulses varied in time. The sinusoidally phase-modulated light (with or without propagation through dispersion compensating fiber) was reflected from the fabricated phase-shifted Bragg grating and directed by a circulator to a photodiode and a sampling oscilloscope with a bandwidth of 50 GHz for diagnostic purposes. Figure 8 shows the spectrum of the sinusoidally phase

#75835 - $15.00 USD Received 12 October 2006; revised 6 December 2006; accepted 12 December 2006

modulated laser radiation for a modulation frequency of f_m = 1 GHz and a modulation index A = 2.405 rad, as measured by an optical spectrum analyzer. The *total* signal bandwidth is estimated to be ≈ 0.1 nm (≈ 12 GHz). Note that the resolution of the spectrum analyzer (0.01 nm) was insufficient to observe the discrete signal spectrum as shown in Fig. 4(b). For the same reason, the dip in Fig. 8 does not reach the expected zero value as in Fig. 4(b). . We measured the response of the spectrum analyzer on the laser line (without modulation) with a width of about 200 MHz and then used this spectral characteristic for the calculation of the spectrum that would be recorded by the spectrum analyzer (instead of the discrete spectrum). From the comparison between the calculated and measured continuous spectra, we obtained the experimental value of the modulation index A given above

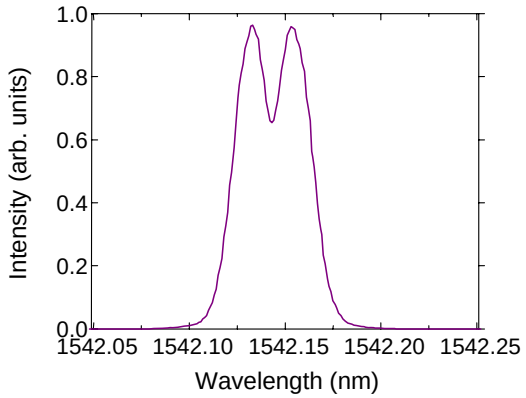

Fig. 8. Measured energy spectrum of the sinusoidally phase modulated laser radiation used as an input signal for optical differentiation.

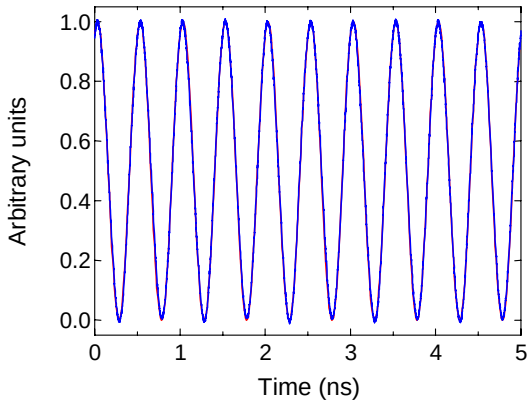

Fig. 9. Numerically calculated squared magnitude of the time derivative of the sinusoidally phase modulated CW light (red curve) and experimentally measured temporal intensity of the output signal after reflection from the phase-shifted fiber Bragg grating (blue curve).

Figure 9 shows the calculated (ideal) time derivative of the sinusoidally phase modulated cw light (red curve) and the measured temporal waveform after reflection of the experimental

#75835 - $15.00 USD Received 12 October 2006; revised 6 December 2006; accepted 12 December 2006

phase modulated light from the phase-shifted FBG (blue curve). There is a remarkable agreement between the theoretical and the experimental derivative curves.

Regarding the second set of experiments, the input pulses to the optical differentiator were formed by propagating the phase modulated light (for f_m = 1 GHz and A = 2.405 rad) through a suitable span of dispersion compensating fiber providing a total dispersion of -4074 ps/nm. The spectrum of the generated pulse train is identical to that of the phase modulated light shown in Fig. 8 (dispersion does not affect the signal energy spectrum), i.e. the total signal bandwidth is again ≈ 12 GHz. The temporal intensity of the pulses at the output of the dispersive fiber is shown in Fig. 10 (blue curve). For comparison, we also show in Fig. 10 the calculated pulses (red curve) assuming the same parameters as in the experiment. Again there is an excellent agreement between the theoretical and experimental results. Finally, Fig. 11 presents the results of differentiation of the optical pulses shown in Fig. 10.

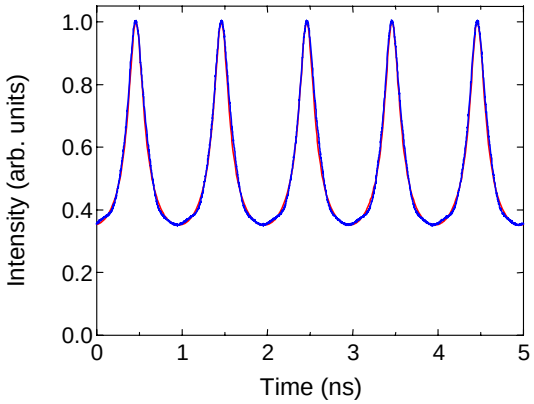

Fig. 10. Experimentally measured (blue curve) and numerically calculated (red curve) temporal intensity of the input pulses formed by sinusoidal phase modulation of CW laser light followed by propagation through a section of dispersion compensating fiber, with the parameters given in the text.

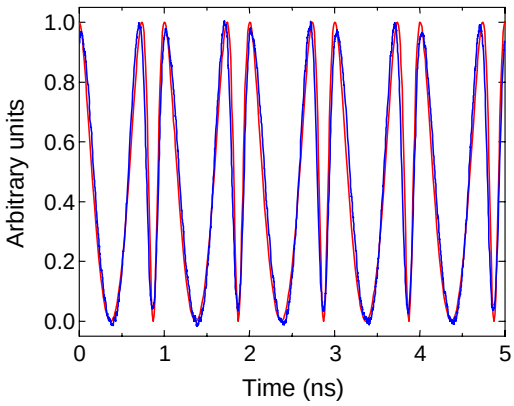

Fig. 11. Numerically calculated squared magnitude of the time derivative (red curve) of the pulses shown in Fig. 10 and experimentally measured intensity of the pulses reflected from the phase-shifted fiber Bragg grating (blue curve).

#75835 - $15.00 USD Received 12 October 2006; revised 6 December 2006; accepted 12 December 2006

Specifically, the exact time derivative of the calculated pulses in Fig. 11 is shown with a red curve whereas the measured signal after reflection from the phase-shifted FBG is shown with a blue curve. The theoretical and experimental curves are again almost identical. For completeness, the energetic efficiency of the differentiation process (ratio between the output and input average optical power) in this last experiment was measured to be ≈ 3%.

6. Conclusions

A very simple and efficient all-optical (all-fiber) first-order temporal differentiation technique based on the use of a single phase-shifted FBG has been proposed and experimentally demonstrated. This device can calculate the first temporal derivative of the complex envelope (amplitude and phase) of arbitrary optical waveforms with bandwidths up to a few gigahertz (sub-nanosecond temporal features). In particular, the specific FBG-based optical differentiator reported here provides an operation bandwidth of ≈ 12 GHz and its accurate performance has been proved by processing two different GHz-bandwidth optical waveforms, namely a phase-only temporal variation and an optical pulse train.

The development of temporal differentiators in the optical domain should prove very useful for all-optical information processing and computing, ultrafast sensing and control using optical signals as well as for implementing specific signal analysis and processing tasks over ultra-wideband microwave waveforms.

Acknowledgments

The authors thank Dr. Yongwoo Park for useful discussions during the preliminary stages of this work.

This research was supported in part by the Natural Sciences and Engineering Research Council of Canada (NSERC), and by the Fonds Québécois de la Recherche sur la Nature et des Technologies (FQRNT).

#75835 - $15.00 USD Received 12 October 2006; revised 6 December 2006; accepted 12 December 2006